

Magnetic vs Inverse Magnetic Catalysis in Hot and Dense Quark Matter

Pavel Slepov

Based on papers

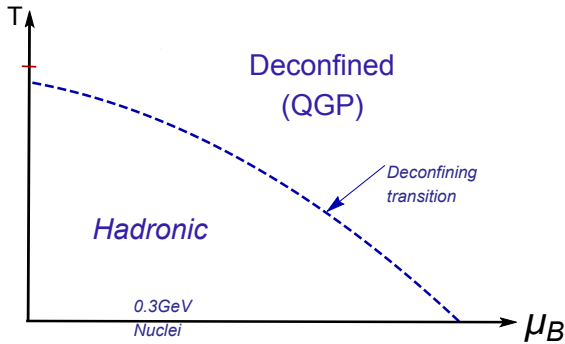
arXiv:2305.06345; Eur. Phys.J.C 83 1, 79, 2023 (arXiv:2203.12539);
JHEP 07, 161, 2021 (arXiv:2011.07023)
with I.Ya.Aref'eva, A. Ermakov, A. Hajilou and K. Rannu

Steklov Mathematical Institute of RAS

*XII International Conference on New Frontiers in Physics
OAC, Kolymbari, Crete, 20. 07. 2023*

QCD Phase Diagram: Early Conjecture

Cabibbo and Parisi, 1975



- μ is a measure of the imbalance between quarks and antiquarks in the system

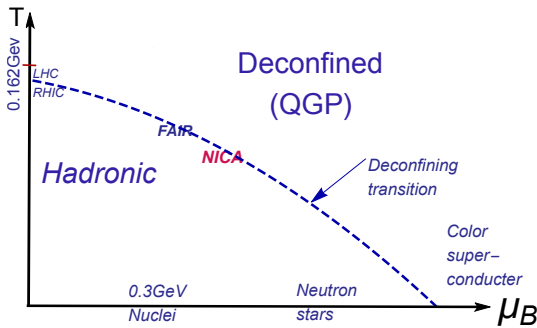
QCD Phase Diagram: Experiments

- LHC, RHIC (2005);
- FAIR (Facility for Antiproton and Ion Research),

NICA (Nuclotron-based Ion Collider fAcility)

Main goals

- search for signs of the phase transition between hadronic matter and QGP;
- search for new phases of baryonic matter

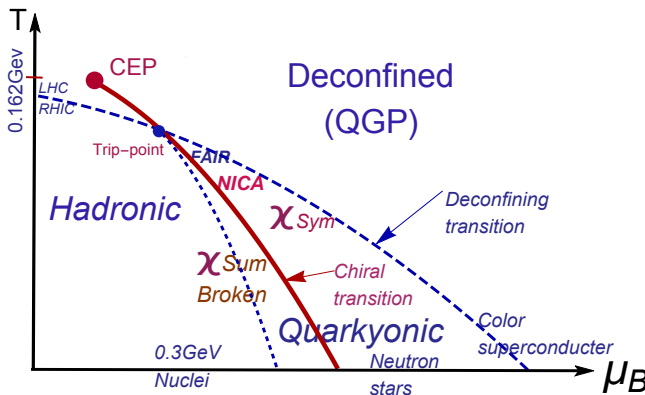


The Expected QCD Phase Diagram

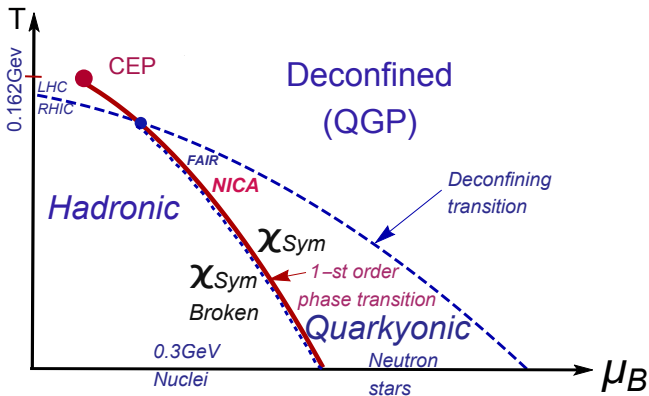
Goal of Holographic QCD — describe QCD phase diagram

Requirements:

- reproduce the QCD results from perturbation theory at short distances
- reproduce Lattice QCD results at large distances (~ 1 fm) and **small μ_B**

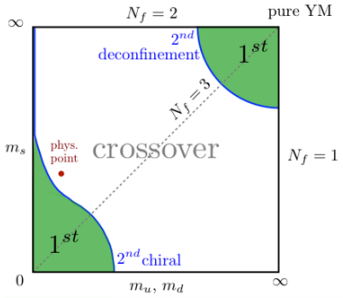


The Expected QCD Phase Diagram

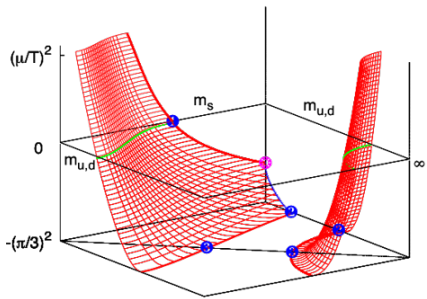


QCD Phase Diagram: Lattice

Phase diagram
on quark mass



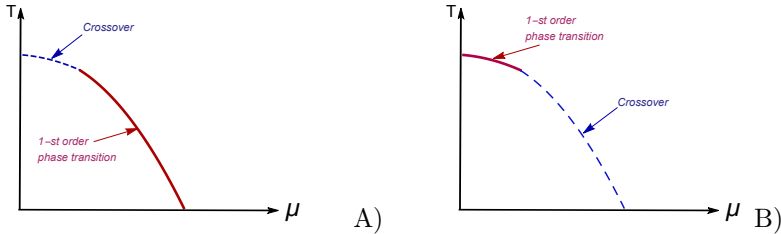
Main problem with $\mu \neq 0$
Imaginary chemical potential method



Columbia plot
Brown et al., PRL, 1990

Philipsen, Pinke, PRD, 2016

“Light” and “Heavy” Quarks from Columbia Plot



The schematic picture of the phase diagrams structure:

A) for light quarks and B) for heavy quarks

Holographic method - phenomenological approach

Perturbation methods are not applicable

Lattice methods do not work, because we consider the process in real time.

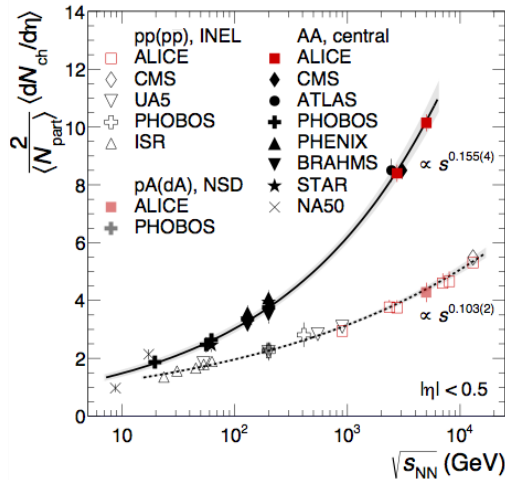
In the stationary case, problems with the chemical potential.

Motivated by AdS/CFT duality

Maldacena, 1998

- Temperature in QCD \iff black hole temperature in (deform.) AdS_5
- Thermalization in QCD \iff formation of black hole in (deform.) AdS_5
- Thermalization models (black hole formation models): colliding shock waves; the area of the trapped surface determines the multiplicity

Total multiplicity produced in heavy ions collision



Plot from PRL'16
(ALICE)
PbPb
 $\mathcal{M} \sim s_{NN}^{0.15}$

The bulk of the particles are born immediately after the collision of heavy ions

Multiplicity

- Experiment

$$\mathcal{M} \sim s^{0.155}$$

- Macroscopic theory of high-energy collisions

$$Landau : \quad \mathcal{M} \sim s^{0.25}$$

- Holographic approach

- The simplest model gives (collision of shock waves)

$$AdS : \quad \mathcal{M} \sim s^{0.33}$$

Gubser et al, Phys.Rev. D, 2008; Gubser et al, JHEP, 2009; Alvarez-Gaume et al, PLB; 2009 Aref'eva et al, JHEP, 2009, 2010, 2012; Lin, Shuryak, JHEP, 2009, 2011; Kiritsis, Taliotis, JHEP, 2011

- Anisotropic Lifshitz type background with exponent ν

$$\begin{aligned}\mathcal{M}_\nu &\sim s^{\frac{1}{2+\nu}}, \\ \mathcal{M}_{LHC} &\sim s^{0.155} \quad \nu = 4.45\end{aligned}$$

Aref'eva, Golubtsova, JHEP, 2014

Holographic model of an anisotropic plasma in a magnetic field at a nonzero chemical potential

Aref'eva, Rannu, P.S., JHEP, 2021

$$S = \int d^5x \sqrt{-g} \left[R - \frac{f_1(\phi)}{4} F_{(1)}^2 - \frac{f_2(\phi)}{4} F_{(2)}^2 - \frac{f_B(\phi)}{4} F_{(B)}^2 - \frac{1}{2} \partial_M \phi \partial^M \phi - V(\phi) \right]$$

$$ds^2 = \frac{L^2}{z^2} \mathfrak{b}(z) \left[-g(z) dt^2 + dx^2 + \left(\frac{z}{L} \right)^{2-\frac{2}{\nu}} dy_1^2 + e^{c_B z^2} \left(\frac{z}{L} \right)^{2-\frac{2}{\nu}} dy_2^2 + \frac{dz^2}{g(z)} \right]$$

$$A_{(1)M} = A_t(z) \delta_M^0 \quad F_{(2)} = dy^1 \wedge dy^2 \quad F_{(B)} = dx \wedge dy^1$$

$$A_t(0) = \mu \quad g(0) = 1 \quad \text{Dudal et al., 2019}$$

$$A_t(z_h) = 0 \quad g(z_h) = 0 \quad \phi(z_0) = 0 \rightarrow \sigma_{\text{string}}$$

Giataganas, 2013; Aref'eva, Golubtsova, 2014 Gürsoy, Järvinen et al., 2019

$$\mathfrak{b}(z) = e^{2\mathcal{A}(z)} \rightarrow \text{quarks mass} \quad \text{“Bottom-up approach”}$$

$$\begin{aligned} \mathcal{A}(z) &= -cz^2/4 \rightarrow \text{heavy quarks background (b, t)} & \text{Andreev, Zakharov, 2006} \\ \mathcal{A}(z) &= -a \ln(bz^2 + 1) \rightarrow \text{light quarks background (d, u)} & \text{Li, Yang, Yuan, 2017} \end{aligned}$$

Holographic model of an anisotropic plasma in a magnetic field at a nonzero chemical potential

$$-\nabla_M \nabla^M \phi + V'(\phi) + \sum_{i=1,2,B} \frac{f'_i(\phi)}{4} F_{(i)}^2 = 0,$$

$$\partial_M (\sqrt{-g} f_i F_{(i)}^{MN}) = 0 \quad \text{no summation on } i, \quad i = 1, 2, B,$$

$$G_{MN} = T_{MN},$$

$$T_{MN} = \sum_{i=1,2,B} T_{MN}^{(A_{(i)})} + T_{MN}^{(\phi)},$$

$$T_{MN}^{(\phi)} = \frac{1}{2} (\partial_M \phi \partial_N \phi - \frac{1}{2} g_{MN} \partial_K \phi \partial^K \phi) - \frac{1}{2} g_{MN} V(\phi),$$

$$T_{MN}^{(A_{(i)})} = \frac{1}{2} f_i \left(F_{(i)ML} F_{(i)N}{}^L - \frac{1}{4} g_{MN} F_{(i)}^2 \right).$$

Holographic anisotropic model for Light Quarks

$$g = e^{c_B z^2} \left[1 - \frac{I_1(z)}{I_1(z_h)} + \frac{\mu^2 (2c - c_B) I_2(z)}{L^2 \left(1 - e^{(2c - c_B)z_h^2/2} \right)^2} \left(1 - \frac{I_1(z)}{I_1(z_h)} \frac{I_2(z_h)}{I_2(z)} \right) \right],$$

$$I_1(z) = \int_0^z \left(1 + b\xi^2 \right)^{3a} e^{-3c_B \xi^2/2} \xi^{1+\frac{2}{\nu}} d\xi, \quad I_2(z) = \int_0^z \left(1 + b\xi^2 \right)^{3a} e^{(c-2c_B)\xi^2} \xi^{1+\frac{2}{\nu}} d\xi,$$

$$A_t = \mu \frac{e^{(2c - c_B)z^2/2} - e^{(2c - c_B)z_h^2/2}}{1 - e^{(2c - c_B)z_h^2/2}}, \quad f_B = -2 \left(\frac{z}{L} \right)^{-2/\nu} e^{-cz^2/2} g \left(\frac{3cz}{2} + \frac{2}{\nu z} - c_B z - \frac{g'}{g} \right),$$

$$f_2 = 2 \left(\frac{z}{L} \right)^{2-4/\nu} \frac{e^{c_B z^2} (\nu - 1)}{\nu^2 z^2 (1 + bz^2)^{2a}} \left((2 + 2\nu - \nu c_B z^2 + \frac{6ab\nu z^2}{1 + bz^2}) g - g' \nu z \right),$$

$$\phi = \int_{z_0}^z \sqrt{\frac{4(\nu - 1)}{\nu^2 \xi^2} - 2c_B \left(3 - \frac{2}{\nu} \right) - 2c_B^2 \xi^2 + \frac{12ab}{1 + b\xi^2} \left(1 + 2 \frac{1 + ab\xi^2}{1 + b\xi^2} \right)} d\xi,$$

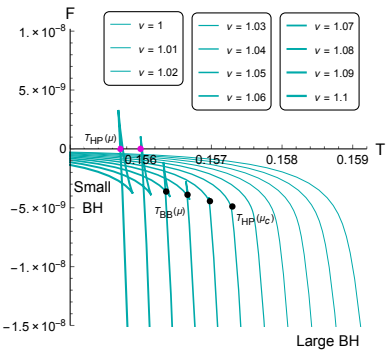
$$V(z) = -\frac{(1 + bz^2)^{2a} z}{2L^2}$$

$$\times \left[2 \left\{ 2 \frac{(1 + \nu)(1 + 2\nu) + (2 + (2 + 3a)(3 + 2\nu)\nu)bz^2 + (1 + \nu + 3a\nu)(1 + 2\nu + 6a\nu)b^2 z^4}{(1 + bz^2)^2 \nu^2 z^2} \right. \right. \\ \left. \left. - c_B \left(2 + \frac{3}{\nu} + \frac{12abz^2}{1 + bz^2} \right) + c_B^2 z^2 \right\} g z - \left(5 + 3 \left(\frac{6ab}{1 + bz^2} - c_B \right) z^2 + \frac{4}{\nu} \right) g' + g'' z \right].$$

Thermodynamics for light quarks model

Temperature T and free energy $F(T)$ for $\mu = 0$

$$T = \frac{|g'|}{4\pi} \Big|_{z=z_h} \quad s = \left(\frac{L}{z_h} \right)^{1+\frac{2}{\nu}} \frac{(1+bz_h^2)^{-3a}}{4} \quad F = \int_{z_h}^{z_{h2}} s \, dT = \int_{z_h}^{z_{h2}} s \, T' \, dz$$

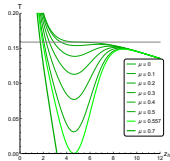


$$\mu = 0,$$

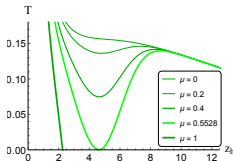
$$c_B = 0$$

Origin of 1-st order phase transition in HQCD

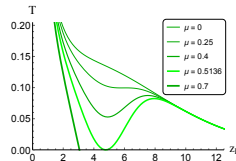
Light quarks, $\nu = 1$



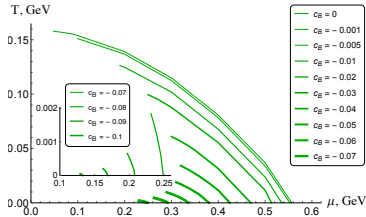
$$c_B = 0$$



$$c_B = 0.001$$

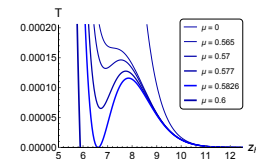
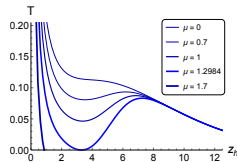
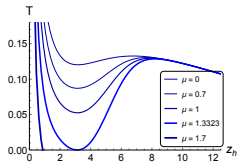


$$c_B = 0.01$$



Origin of 1-st order phase transition in HQCD

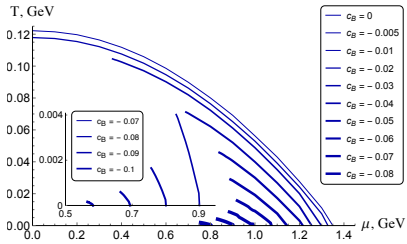
Light quarks, $\nu = 4.5$



$$c_B = 0$$

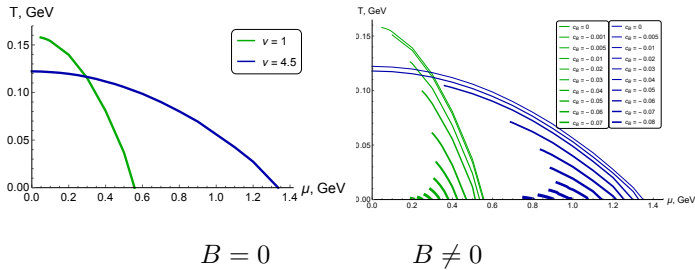
$$c_B = 0.001$$

$$c_B = 0.01$$



Comparison of the 1-st order phase transition

Phase transitions of the 1st order in isotropic (green lines $\nu = 1$) and anisotropic (blue lines $\nu = 4.5$) models



- For $B = 0$, the onset of the 1st order PTs moves towards $\mu = 0$ as ν increases
- As c_B increases (strong magnetic field) phase transition line lengths decrease

Modified warp-factor and holographic anisotropic model for Heavy Quarks

NEW Warp-factor:

$$\mathcal{A}(z) = -cz^2/4 - (p - c_B q_3)z^4$$

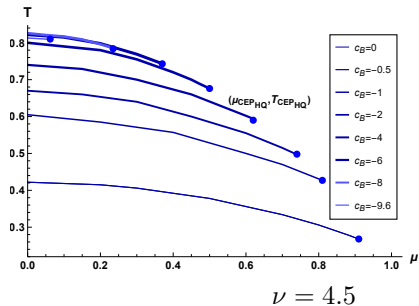
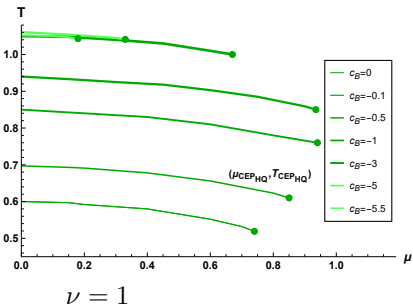
Aref'eva, Hajilou, Rannu and P. S., arXiv:2305.06345

$$g(z) = e^{c_B z^2} \left[1 - \frac{\tilde{I}_1(z)}{\tilde{I}_1(z_h)} + \frac{\mu^2 (2R_{gg} + c_B(q_3 - 1)) \tilde{I}_2(z)}{L^2 \left(1 - e^{(2R_{gg} + c_B(q_3 - 1)) \frac{z_h^2}{2}} \right)^2} \left(1 - \frac{\tilde{I}_1(z)}{\tilde{I}_1(z_h)} \frac{\tilde{I}_2(z_h)}{\tilde{I}_2(z)} \right) \right],$$

$$\tilde{I}_1(z) = \int_0^z e^{(2R_{gg} - 3c_B) \frac{\xi^2}{2} + 3(p - c_B q_3) \xi^4} \xi^{1+\frac{2}{\nu}} d\xi,$$

$$\tilde{I}_2(z) = \int_0^z e^{\left(2R_{gg} + c_B \left(\frac{q_3}{2} - 2\right)\right) \xi^2 + 3(p - c_B q_3) \xi^4} \xi^{1+\frac{2}{\nu}} d\xi.$$

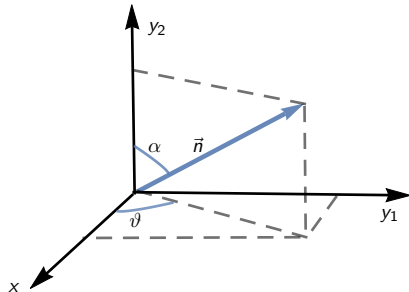
The 1-st order phase transition in HQCD with modified warp-factor for Heavy Quarks



Temporal Wilson loops in fully anisotropic background

$$S = \frac{1}{2\pi\alpha'} \int dt d\xi \sqrt{-\det h_{\alpha\beta}}, \quad h_{\alpha\beta} = G_{MN} \partial_\alpha X^M \partial_\beta X^N.$$

$$\begin{aligned} X^0 &\equiv t, & X^1 &\equiv x = \xi \cos \vartheta \sin \alpha, & X^2 &\equiv y_1 = \xi \sin \vartheta \sin \alpha, \\ X^3 &\equiv y_2 = \xi \cos \alpha, & && X^4 &\equiv z = z(\xi). \end{aligned}$$



Temporal Wilson loops in fully anisotropic background

The Nambu-Goto action is

$$S = -\frac{\tau}{2\pi\alpha'} \mathcal{S}, \quad \mathcal{S} = \int_{-\ell/2}^{\ell/2} d\xi M(z(\xi)) \sqrt{\mathcal{F}(z(\xi)) + (z'(\xi))^2},$$
$$M(z(\xi)) = \frac{\mathfrak{b}_s(z(\xi))}{z^2(\xi)}, \quad \tau = \int d\xi^0,$$
$$\mathcal{F}(z(\xi)) = g(z(\xi^1)) (\mathfrak{g}_1 \cos^2 \vartheta \sin^2 \alpha + \mathfrak{g}_2 \sin^2 \vartheta \sin^2 \alpha + \mathfrak{g}_3 \cos^2 \alpha),$$

\mathfrak{g}_i - anisotropy functions. Let's introduce the effective potential

$$\mathcal{V}(z(\xi)) \equiv M(z(\xi)) \sqrt{\mathcal{F}(z(\xi))} =$$
$$= \frac{\mathfrak{b}_s(z(\xi))}{(z^2(\xi))} \sqrt{g(z(\xi)) (\mathfrak{g}_1 \cos^2 \vartheta \sin^2 \alpha + \mathfrak{g}_2 \sin^2 \vartheta \sin^2 \alpha + \mathfrak{g}_3 \cos^2 \alpha)},$$

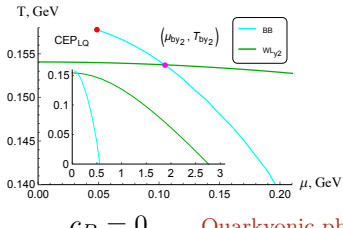
$\mathcal{V}'(z)|_{z=z_{DW}} = 0$, z_{DW} is the dynamical wall point and for string tension:

$$\sigma_{DW} = M(z_{DW}) \sqrt{\mathcal{F}(z_{DW})}$$

Andreev, Zakharov PRD'06 Aref'eva'16 Aref'eva, Rannu, P.S., PLB'19.

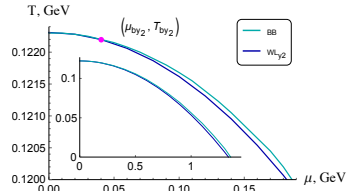
Phase transitions for light quarks

isotropic, $\nu = 1$

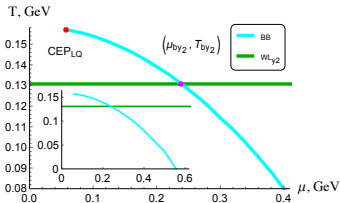


$$c_B = 0$$

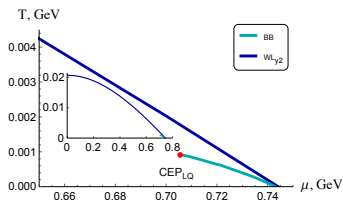
anisotropic, $\nu = 4.5$



Quarkyonic phase (QP) appears during isotropization



$$c_B = -0.0000985$$

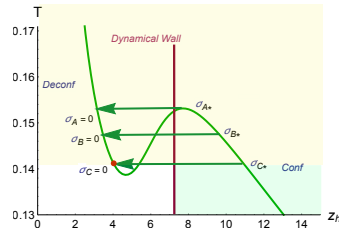
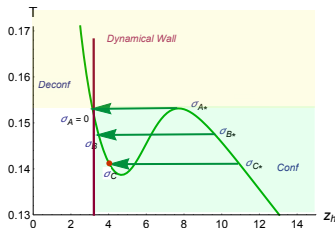


$$c_B = -0.0858$$

For $\nu = 4.5$ QP appears at large magnetic field and large μ

Background 1-st order PT \Rightarrow 1-st order PT for physical quantities

- Physical quantities that probe backgrounds are smooth relative to z_h
 \Rightarrow their dependence on T **should be taken from stable region**
- BB-PT immediately provides the 1-st PT for corresponding characteristic of QCD



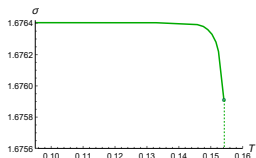
The arrows show transitions from the unstable phases to the stable ones

Plots for $\sigma(T)$ and different boundary conditions.

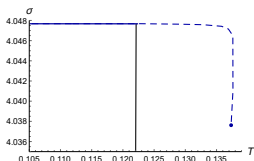
$$z_0 = 0.1, \quad c_B = 0$$

$\mu = 0:$

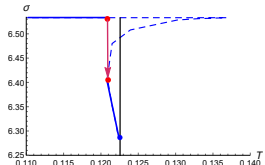
dashed for unstable phase



$\nu = 1$

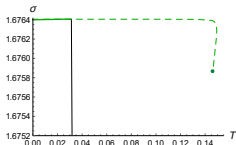


$\nu = 4.5, \vartheta = 0^0$

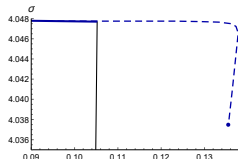


$\nu = 4.5 \vartheta = 90^0$

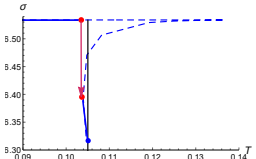
$\mu = 0.5:$



$\nu = 1$



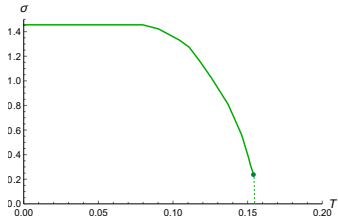
$\nu = 4.5, \vartheta = 0^0$



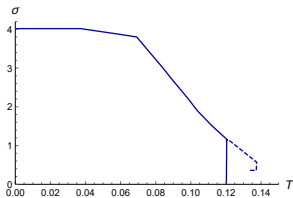
$\nu = 4.5 \vartheta = 90^0$

Plots for $\sigma(T)$ and different boundary conditions.

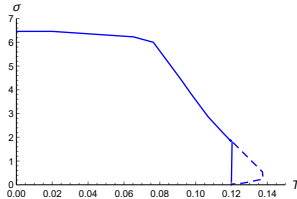
$$z_0 = 10 \exp(-z_h/4) + 0.1, \quad c_B = 0$$



$$\mu = 0, \nu = 1$$



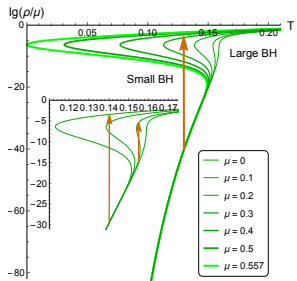
$$\mu = 0.2, \nu = 4.5, \vartheta = 0^0$$



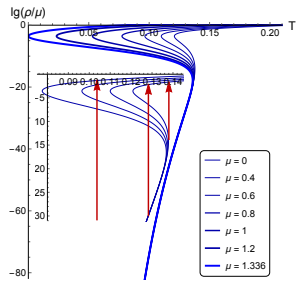
$$\mu = 0.2, \nu = 4.5, \vartheta = 90^0$$

Change of Density across the 1-st Order Transition

$$A_t(z) = \mu - \rho z^2 + \dots$$



$\nu = 1$



$\nu = 4.5$

Density $\rho/\mu(T)$ in logarithmic scale for different μ
 $a = 4.046, b = 0.01613, c = 0.227$

Inner plots show the fragments of main plots zoomed

- At a given T the value of the ratio ρ/μ increases with the transition from unstable to stable state. **Quarkionic phase transition?**

Electrical conductivity and photon emission rate

The number of photons emitted per unit time per unit volume Γ (photon emission rate) in thermal equilibrium is given by the light-like correlator

$$d\Gamma = -\frac{d\mathbf{k}}{(2\pi)^3} \frac{e^2 n_b(|\mathbf{k}|)}{|\mathbf{k}|} \text{Im} [\eta_{\mu\nu} G_R^{\mu\nu}]_{k^0=|\mathbf{k}|},$$

$$n_b(|\mathbf{k}|) = \frac{\mathcal{A}}{e^{-|\mathbf{k}|/T} - 1}$$

is Bose-Einstein thermal distribution function, $\eta_{\mu\nu}$ is Minkowski metric tensor, photon's 4-momentum is $k^\mu = (k^0, \mathbf{k})$. Note that the retarded Green's function $G_R^{\mu\nu}$ is related to the electric conductivity through the Kubo relation

$$\sigma^{\mu\nu} = -\frac{G_R^{\mu\nu}}{iw},$$

so the direct photons emission rate is connected to the conductivity of QGP.
The spectral density $\chi^{\mu\nu}(k) = -2 \text{Im}[G_R^{\mu\nu}(k)]$

Polarization

The spatial polarization four-vectors $\epsilon_\mu^{(s)}$: \perp to k , i.e. $\epsilon_i^{(s)} k_j \delta^{ij} = 0$, $s = 1, 2$ $\epsilon_i^{(1)} \epsilon_j^{(2)} \delta^{ij} = 0$.

Coordinate system: \vec{B} along the z -direction, i.e. $F = B dx \wedge dy$ Reaction plane: (xy -plane)

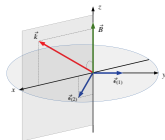
If there is a rotational symmetry on the xy plane then we take \vec{k} belong xz -plane

ϑ is the angle between \vec{k} and \vec{B} .

Wave and polarization four-vectors take the form

$$k_\mu = k_0(1, \sin \vartheta, 0, \cos \vartheta), \quad \epsilon_\mu^{(1)} = (0, 0, 1, 0), \quad \epsilon_\mu^{(2)} = (0, \cos \vartheta, 0, -\sin \vartheta),$$

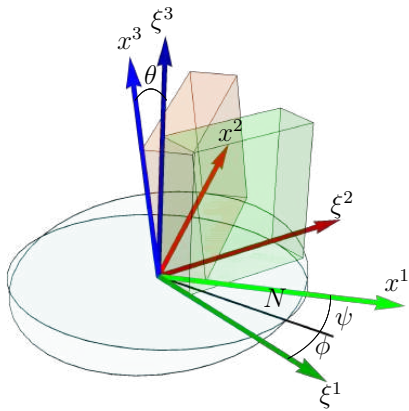
Decomposition of the rate of emitted photons



$$\frac{d\Gamma}{d\vec{k}} = \sum_{s=1,2} \frac{d\Gamma_s}{d\vec{k}}, \quad \frac{d\Gamma_s}{d\vec{k}} = \frac{e^2}{(2\pi)^3 2|\vec{k}|} n_B(k^0) \epsilon_\mu^{(s)}(\vec{k}) \epsilon_\nu^{(s)}(\vec{k}) \chi^{\mu\nu}(k) \Big|_{k=0},$$

$$\frac{d\Gamma_1}{d\vec{k}} \propto \chi^{22}, \quad \frac{d\Gamma_2}{d\vec{k}} \propto \cos^2 \vartheta \chi^{11} - 2 \cos \vartheta \sin \vartheta \chi^{13} + \sin^2 \vartheta \chi^{33}$$

Polarization



The green slab shows orientation axes related with HIC geometry:
 ξ^1 along collision line,
 ξ^2 along the orientation of the impact parameter
 ξ^3 along the direction of the magnetic field.

Rotating the green plate by the Euler angles (ϕ, θ, ψ) , we obtain a pink plate oriented along the axes (x^1, x^2, x^3) , coinciding with the vector \vec{k} and polarization vectors $\epsilon_{(1)}^\mu$ and $\epsilon_{(2)}^\mu$

Polarization

$$k_1 = a_{31}(\phi, \theta, \psi) = \sin \phi \sin \theta,$$

$$k_2 = a_{32}(\phi, \theta, \psi) = \cos \phi \sin \theta,$$

$$k_3 = a_{33}(\phi, \theta, \psi) = \cos \theta$$

$$\epsilon_1^{(1)} = a_{21}(\phi, \theta, \psi) = \cos \theta \cos \psi \sin \phi + \cos \phi \sin \psi,$$

$$\epsilon_2^{(1)} = a_{22}(\phi, \theta, \psi) = \cos \phi \cos \theta \cos \psi - \sin \phi \sin \psi,$$

$$\epsilon_3^{(1)} = a_{23}(\phi, \theta, \psi) = -\cos \psi \sin \theta,$$

$$\epsilon_1^{(2)} = a_{11}(\phi, \theta, \psi) = \cos \phi \cos \psi - \cos \theta \sin \phi \sin \psi,$$

$$\epsilon_2^{(2)} = a_{12}(\phi, \theta, \psi) = -\cos \psi \sin \phi - \cos \phi \cos \theta \sin \psi,$$

$$\epsilon_3^{(2)} = a_{13}(\phi, \theta, \psi) = \sin \theta \sin \psi$$

Compare with previous case: Wave and polarization four-vectors take the form

$$k_\mu = k_0(1, \sin \phi \sin \vartheta, \cos \phi \sin \vartheta, \cos \vartheta),$$

$$\epsilon_\mu^{(1)} = (0, 0, 1, 0), \quad \epsilon_\mu^{(2)} = (0, \cos \vartheta, 0, -\sin \vartheta),$$

Polarization

$$\frac{d\Gamma_s}{d\vec{k}} = \frac{e^2}{(2\pi)^3 2|\vec{k}|} n_B(k^0) \epsilon_m^{(s)}(\vec{k}) \epsilon_n^{(s)}(\vec{k}) \chi^{mn}(k) \Big|_{k=0}$$

$$\begin{aligned}\frac{d\Gamma_1}{d\vec{k}} &\propto \chi^{11} (\cos(\theta) \cos(\psi) \sin(\phi) + \cos(\phi) \sin(\psi))^2 \\ &+ \chi^{22} (\cos \phi \cos \theta \cos \psi - \sin \phi \sin \psi)^2 + \chi^{33} (\cos \psi \sin \theta)^2\end{aligned}$$

$$\begin{aligned}\frac{d\Gamma_2}{d\vec{k}} &\propto \chi^{11} (\cos \phi \cos \psi - \cos \theta \sin \phi \sin \psi)^2 \\ &+ \chi^{22} (-\cos \psi \sin \phi - \cos \phi \cos \theta \sin \psi)^2 + \chi^{33} (\sin \theta \sin \psi)^2\end{aligned}$$

Electrical conductivity for light quarks

To investigate properties of direct photons in heavy-ion collisions using holographic duality one has to introduce one more Maxwell field:

$$S_{out} = -\frac{1}{4} \int d^5x \sqrt{-g} f_0 F_{MN} F^{MN},$$

$f_0 = f_0(\phi)$ is the function of coupling of the Maxwell field to the dilaton. To find the electric conductivity, we add a probe Maxwell field to action. Consider an ansatz for this probe field in the form of a plane wave propagating in x_3 direction

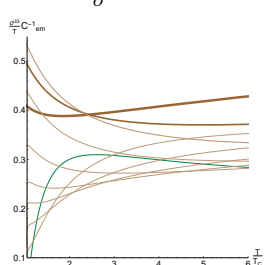
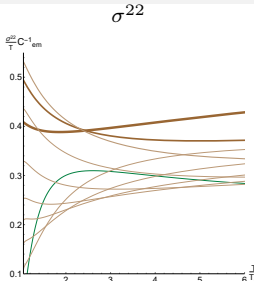
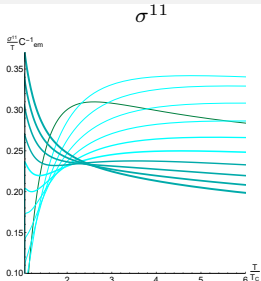
$$A_M(t, x_3, z) = \psi_M(z) \exp(-i(wt - kx_3)), \quad M = 0, \dots, 4.$$

Using the Kubo formula $\sigma^{\mu\nu} = -G_R^{\mu\nu}/iw$ we obtain:

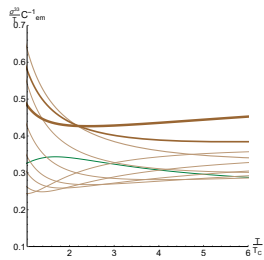
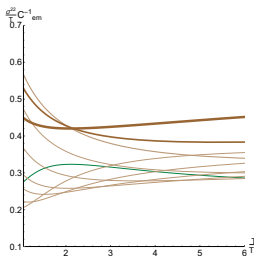
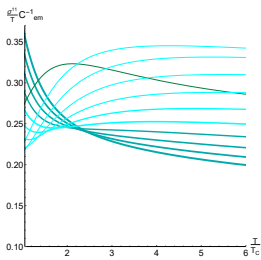
$$\begin{aligned} \sigma^{11} &= \frac{2f_0(z_h)}{z_h} \sqrt{\frac{\mathfrak{b}(z_h)\mathfrak{g}_3(z_h)\mathfrak{g}_2(z_h)}{\mathfrak{g}_1(z_h)}}, \quad \sigma^{22} = \frac{2f_0(z_h)}{z_h} \sqrt{\frac{\mathfrak{b}(z_h)\mathfrak{g}_3(z_h)\mathfrak{g}_1(z_h)}{\mathfrak{g}_2(z_h)}} \\ \sigma^{33} &= \frac{2f_0(z_h)}{z_h} \sqrt{\frac{\mathfrak{b}(z_h)\mathfrak{g}_1(z_h)\mathfrak{g}_2(z_h)}{\mathfrak{g}_3(z_h)}} \end{aligned}$$

Electrical conductivity for light quarks

$$\mu = 0 \\ c_B = 0$$



$$\mu = 0.5 \\ c_B = 0.05$$



$\nu = 1$ (darker green), $\nu = 1.05, 1.1, 1.15, 1.2, 1.3, 1.5, 2, 3, 4.5$

- μ и магнитное поле B для всех σ^{ii} уменьшают "распространение" анизотропии

Properties of an anisotropic plasma in a magnetic field at a nonzero chemical potential

- Energy losses \iff tension of the spatial Wilson loop
 - heavy quarks, $B \neq 0$
Aref'eva, Rannu, P.S.
 - light quarks, $B \neq 0$
in progress
- Jets quenching \iff Wilson loop in lightlike direction
 - heavy quarks, $B = 0$
Aref'eva et al, Nucl.Phys.B, 2018
 - light quarks, $B \neq 0$
in progress
- Photon emission and electrical conduction
Aref'eva, Ermakov, Rannu, P.S., EPJC22, arXiv:2203.12539
- Entanglement entropy and the number of particles born in a selected volume
 - Aref'eva, Phys.Part.Nucl.Lett.'19
 - Aref'eva, Patrushev, P.S., JHEP'20

$$d\Gamma \sim \text{Im} [\text{tr} (\eta_{\mu\nu} G_R^{\mu\nu})]_{k^0=|\mathbf{k}|}, \quad \sigma^{\mu\nu} = -\frac{G_R^{\mu\nu}}{iw}$$

Conclusion

- We have reproduced (using holography) experimental dependence of total particle multiplicity on energy
- QCD phase diagram
 - Anisotropy leads to smearing of the confinement/deconfinement phase transition
 - Magnetic field dependence – effect of inverse/direct magnetic (MC) catalysis:
 - Dependence on quark mass: **for heavy quarks should be MC (for improved holographic model is OK), for light quarks – IMC (OK)**
- Dependence of electrical conductivity on
 - anisotropy
 - quark masses: σ^{11} weak, σ^{22}, σ^{33} essential dependencies
 - magnetic field - reduces anisotropy smearing
- We expect a jump of electrical conductivity and photon emission rate near the 1-st order phase transition.
- For some parameters of anisotropy and magnetic field we can define the new phase with significantly different values of string tension, baryonic density and electrical conductivity, but this phase is still located in the confinement zone. This phase can be interpreted as a quarkyonic phase.

Thank you for your attention!